Atmospheric CO_2 and CH_4 abundances on regional scales in boreal areas using CAMS reanalysis, COCCON spectrometers and Sentinel-5 Precursor satellite observations

Qiansi Tu[1], Frank Hase[1], Thomas Blumenstock[1], Rigel Kivi[2], Pauli Heikkinen[2], Mahesh Kumar Sha[3],
Uwe Raffalski[4], Jochen Landgraf[5], Alba Lorente[5], Tobias Borsdorff[5], Huilin Chen[6]

[1]Karlsruhe Institute of Technology, IMK-ASF, Karlsruhe, Germany
[2]Finnish Meteorological Institute, Sodankylä, Finland
[3]Royal Belgian Institute for Space Aeronomy (BIRA-IASB), Brussels, Belgium
[4]Swedish Institute of Space Physics, Kiruna, Sweden
[5]SRON Netherlands Institute for Space Research, Utrecht, the Netherlands
[6]Centre for Isotope Research, University of Groningen, Groningen, the Netherlands

Correspondence to: Qiansi Tu (qiansi.tu@kit.edu)

Abstract.

We compare the atmospheric column-averaged dry-air mole fractions of carbon dioxide (XCO_2) and methane (XCH_4) measured with a pair of COCCON spectrometers at Kiruna and Sodankylä sites in boreal areas with model data provided by the Copernicus Atmosphere Monitoring Service (CAMS) and with XCH_4 from the recently launched Sentinel-5 Precursor (S5P) satellite. In addition, measured and modeled gradients of XCO_2 and XCH_4 (ΔXCO_2 and ΔXCH_4) on regional scales are investigated. Both sites show a similar and very good correlation between COCCON retrievals and the modeled CAMS XCO_2 data, while CAMS data are biased high with respect to COCCON by 3.72 ppm (±1.80 ppm) in Kiruna and 3.46 ppm (±1.73 ppm) in Sodankylä on average. For XCH_4 CAMS values are higher than the COCCON observations by 0.33 ppb (±11.93 ppb) in Kiruna, and 7.39 ppb (±10.92 ppb) in Sodankylä. In contrast, the S5P satellite generally measures lower atmospheric XCH_4 than the COCCON spectrometers, with a mean difference of 9.69 ppb (±20.51 ppb) in Kiruna and 3.36 ppb (±17.05 ppb) in Sodankylä. We compare the gradients of XCO_2 and XCH_4 (ΔXCO_2 and ΔXCH_4) between Kiruna and Sodankylä derived from CAMS reanalysis and COCCON and S5P measurements to study the capability of detecting sources and sinks on regional scales. The correlations in ΔXCO_2 and ΔXCH_4 between the different datasets are generally smaller than the correlations in XCO_2 and XCH_4 between the datasets at either site. The ΔXCO_2 predicted by CAMS are generally higher than those observed with COCCON with a slope of 0.51. The ΔXCH_4 predicted by CAMS is mostly higher than that observed with COCCON with a slope of 0.65, covering a larger dataset than the comparison between S5P and COCCON. When comparing CAMS ΔXCH_4 with COCCON ΔXCH_4 only in S5P overpass days (slope = 0.53), the correlation is close to that between S5P and COCCON (slope = 0.51). CAMS, COCCON and S5P predict gradients in reasonable agreement. However, the small number of observations coinciding with S5P limits our ability to verify the performance of this sensor. We detect no significant impact of ground albedo and viewing zenith angle on the S5P results. Both sites show similar situation with the average ratio of XCH_4

(S5P/COCCON) of 0.9949 ± 0.0118 in Kiruna and 0.9953 ± 0.0089 in Sodankylä. Overall, the results indicate that the
35 COCCON instrument has the capability of measuring greenhouse gas (GHG) gradients on regional scales and observations
performed with the portable spectrometers can contribute to inferring sources and sinks and to validating space borne
greenhouse gas sensors.

1 Introduction

Carbon dioxide (CO_2) concentrations in the atmosphere are steadily increasing since the industrialisation. This rise is mainly
40 attributed to manmade emissions as consequence of the use of fossil fuels. The 2018 global mean abundance relative to the
year 1750 is 147% (WMO Greenhouse Gases Bulletin, 2019). Methane (CH_4), the second most important anthropogenic
greenhouse gas (GHG) after CO_2, has increased by about 259% since pre-industrial times (WMO Greenhouse Gases Bulletin,
2019). Since GHGs have a major impact on global climate, scientific research is aiming at accurate accounting of GHG
exchanges for achieving a better understanding of the global carbon budget. Satellite measurements of column-averaged
45 greenhouse gas abundances are an important source of information for this research. However, satellite observations at high
latitudes have lower confidence due to the high airmass present in the path of the incoming signal. Because strong responses
to climate change are expected at high latitudes, it is important to obtain accurate observations of GHGs also at high latitudes
with high spatial and temporal coverage. Currently, both satellite and ground-based observations are used to monitor GHGs
column-averaged abundances.

50 Sentinel-5 Precursor (S5P) is the first mission of the Copernicus Programme, aiming to monitor air quality, climate and
ozone abudances with high spatio-temporal resolution and daily global coverage (Veefkind et al., 2012). The mission fills in
the gap in the continuity between SCIAMACHY on board Envisat (Bovensmann, 1999) and Sentinel-5
(https://earth.esa.int/web/guest/missions/esa-future-missions/sentinel-5). The S5P satellite was launched on October 13, 2017
and operates in a low Earth polar orbit, with an operational lifespan of 7 years. Its single payload, the TROPOspheric
55 Monitoring Instrument (TROPOMI) is a nadir-viewing grating spectrometer that covers wavelength bands from ultraviolet to
shortwave infrared (SWIR). TROPOMI measures back-scattered solar radiation spectra using a push-broom configuration
combining a swath width of 2600 km. The instrument features a very high spatial resolution of approximately 5.5×7 km^2 in
the SWIR spectral band at nadir providing global daily coverage. The SWIR module on TROPOMI covers the spectral range
of 4190 to 4340 cm^{-1} (spectral resolution: 0.45 cm^{-1}) and is used to measure the concentration of methane and carbon monoxide
60 in the Earth's atmosphere (Butz et al., 2012; Hu et al., 2018).

To validate the S5P column-averaged CH_4 observations, the ground-based column-averaged CH_4 measurements from solar-
viewing near-infrared spectrometers are comprehensively used (Lambert et al., 2019). The Total Carbon Column Observing
Network (TCCON) is a global network of ground-based Fourier transform infrared (FTIR) spectrometers, measuring solar
absorption spectra in the near infrared region to retrieve column-averaged dry-air mole fractions of CO_2 (XCO_2) and CH_4
65 (XCH_4) amongst other gases (Wunch et al., 2011). The TCCON measurements have high precision because the effect of surface

properties and aerosols on the measurements are minimal (Wunch et al., 2017). The measurements are scaled to the World Meteorological Organization (WMO) reference scale applying a post correction and thereby guaranteeing high accuracy (Wunch et al., 2015). The high-resolution TCCON sites are distributed globally, however, many of these are concentrated in Europe, Northern America and eastern Asia. The costs, logistic requirements and the need of qualified personnel on site have 70 hindered the expansion of the network e.g. to the African continent, South America and central Asia (Wunch et al., 2011). Remote sites and regions with high or low surface albedo are generally poorly covered by the TCCON network. Ground-based measurement stations in the above mentioned regions are needed for satellite and model validation and carbon cycle science.

Recently, cheaper and portable spectrometers have been developed and are now available for GHG measurements, with the potential to complement the TCCON network (Frey et al., 2019; Sha et al., 2019). The EM27/SUN FTIR spectrometer was 75 developed by Karlsruhe Institute of Technology (KIT) (Gisi et al., 2012), in cooperation with Bruker Optics GmbH, Ettlingen, Germany. It is available from Bruker as a commercial device since spring 2014. The EM27/SUN instrument is a portable ground-based FTIR spectrometer, consisting of a spectrometer body with dimensions of $35 \times 40 \times 27$ cm and a solar tracker which is directly mounted on the spectrometer. The whole weight is approximately 25 kg and can be carried by one person. This solar-viewing FTIR instrument has a resolution of 0.5 cm^{-1}, similar to that of TROPOMI. This compact and mobile 80 EM27/SUN instrument is appropriate for field campaigns as well as for long-term deployment at a site with the potential to complement the TCCON network. In addition, its excellent robust and reliable characteristics have been demonstrated in several successful field campaigns (Frey et al., 2015; Klappenbach et al., 2015; Butz et al., 2017; Vogel et al., 2019; Kille et al., 2019; Sha et al., 2019b). KIT performs final optimisations, an expert review of instrument performance and a final calibration of each unit with respect to the reference EM27/SUN spectrometer operated at KIT and the TCCON site in 85 Karlsruhe. In the framework of ESA recent projects, codes required for the data analysis of EM27/SUN measurements have been developed by KIT, which are open source and freely available (https://www.imk-asf.kit.edu/english/3225.php). If the operation of EM27/SUN spectrometers adheres to the described standards (use of calibrated units, processing using the provided codes), then this practice is compatible with the requirements of COCCON (Collaborative Carbon Column Observing Network, see Frey et al., 2019). The data presented in this paper have been generated using a pair of EM27/SUN spectrometers 90 following these requirements. For this reason, we refer to these as COCCON spectrometers in the following. This paper compares S5P observations to the ground-based observations from two COCCON spectrometers operated in the high latitude regions in Sodankylä, Finland and Kiruna, Sweden. The measurements from these two sites are highly valuable for investigating the gradients of the greenhouse gas distribution on regional scales near the Arctic Circle.

In addition to the COCCON and the TROPOMI datasets, we investigate the CO_2 and CH_4 products from Copernicus 95 Atmosphere Monitoring Service (CAMS). CAMS services are operated by the European Centre for Medium-Range Weather Forecasts (ECMWF), providing near-real-time analysis and forecast data with a spatial resolution of approximately 80 km. The CAMS reanalysis dataset is the latest global reanalysis dataset of atmospheric composition, though a reanalysis for the greenhouse gases (CO_2, CH_4) is being produced separately and will only be released in 2019 (Inness et al., 2019). This work uses 6-hourly analyses CAMS data of CO_2 and CH_4, initialized daily from analyses at 00:00 UTC. CAMS profiles of CO_2 and

100 CO$_4$ are also used to study the quality of a-priori profiles used for the trace gas retrievals, and compared with the TCCON official MAP a-priori profiles.

In this study, we provide an intercomparison of atmospheric CO$_2$ and CH$_4$ column-averaged abundances derived from ground-based COCCON spectrometers and the CAMS reanalysis dataset, and CH$_4$ from S5P satellite within the Arctic Circle. Another objective is to explore the ability of the S5P satellite and the COCCON in observing the gradients of GHGs on regional

105 scales in high latitude regions. The following section gives a description of the sites and data sources. The results and discussions are given in section 3 and the final conclusions are discussed in section 4.

2 Sites and data sources

Multi-year measurements using two COCCON spectrometers were performed since March 2017 at the Finnish Meteorological Institute (FMI), Sodankylä, Finland (67.37°N, 26.63°E, 181 m a.s.l.) and at the Swedish Institute of Space Physics (IRF),

110 Kiruna, Sweden (67.84°N, 20.41°E, 419 m a.s.l.). The area around these two sites represents a typical northern boreal forest/taiga environment, surrounded predominantly by coniferous forest with some mixed/deciduous forest. Regular TCCON measurements are performed at the Sodankylä site since 2009 providing XCO$_2$ and XCH$_4$ measurements (Kivi et al., 2016). The COCCON operation at the FMI observational station is performed in the framework of the Fiducial Reference Measurements for Ground-Based Infrared Greenhouse Gas Observations campaign (FRM4GHG,

115 http://frm4ghg.aeronomie.be/) funded by the European Space Agency (ESA). The COCCON measurements at the FMI as part of this campaign started since March 2017 and continued till end of 2019, during which the additional COCCON measurements in Kiruna were performed by KIT and IRF as well.

The public S5P CH$_4$ data are only available since May 2018. The comparison between the S5P and the COCCON measurements starts since the beginning of the public data. Currently, the Level-2 (L2) products of S5P are released, including

120 the column-average dry-air mole fraction of methane, XCH$_4$. This value presents the total column of methane in the atmosphere from the surface up to the top of the atmosphere divided by the corresponding dry-air column (Apituley et al., 2017). S5P L2 products provide bias corrected XCH$_4$ retrievals, which are used in this work. The quality control value (qa_value) is given as part of the CH$_4$ data product and it is recommended use only data with qa value above 0.5 to exclude data of questionable quality. To compare with the COCCON data, S5P data are collected from the average value within a radius of 100 km around

125 each station. The radius criterion of 100 km was the best tested case as discussed in Sha et al., 2019a. When comparing the bias corrected S5P XCH4 product with the NDACC and TCCON FTIR products, it shows slightly higher correlation in using the radius criterion of 100 km than those of using 50 km. A 10-minute average value of COCCON data (retrieved from approximate 10 spectra) is obtained at the coincident S5P overpass time. The overpass time over Kiruna and Sodankylä stations is between 9 UTC to 12 UTC. The standard error of mean is used as error bar, as it presents the estimation of the standard

130 deviation of its sampling distribution and is calculated by using:

$$\varepsilon = \frac{\sqrt{\frac{1}{n}\sum_i (x_i - \bar{x})^2}}{\sqrt{n}},$$ (1)

here the x_i is single measurement in the defined area or time range, $\bar{x}$ is mean value of data sample, n is the number of data points. This method is useful to distinguish highly scattered dataset, especially in S5P and CAMS data, which come from large areas.

135   The comparison between the CAMS reanalysis and the COCCON observations starts from the beginning of the field campaign (March 2017). CAMS provides a 6-hourly reanalysis data in defined areas around Kiruna and Sodankylä. These defined areas resemble rectangles of 100 km × 100 km, covering 67°N – 69°N and 18°E – 23°E around Kiruna; 66.5°N – 68.3°N and 24°E – 29°E around Sodankylä. In these defined areas there are 476 data points in total in the area of Kiruna and 442 data points in the area of Sodankylä within their respective measuring periods. We use the average value from these points

140   as hourly CAMS reanalysis data. The coincident COCCON data are collected from one-hour average at 6 UTC or 12 UTC, because the spectrometer measures only at daytime. Additionally, selection criteria are applied to the COCCON data as described in the work of Frey et al. (2015). Measurements are filtered out as they were measured at solar zenith angle (SZA) > 80° to reduce uncertainties connected to spectra recorded at very high airmasses. The data are also filtered based on Xair (column-averaged amount of dry air) and Xair range between 0.995 and 1.005 is required.

145   Any practical choice of the a-priori volume mixing ratio (VMR) profiles is generally based on model data. To assess the quality of the model data, knowledge of the actual profiles is required and might be obtainable from in-situ instruments onboard aircrafts performing profile measurements or from in-situ AirCore balloon launches. The AirCore, which was an auxiliary activity in the FRM4GHG campaign, is a simple and viable atmospheric sampling system to measure vertical profiles of greenhouse gases (Karion et al., 2010). The AirCore system that was used in Sodankylä was built at the University of

150   Groningen (UG) and at the FMI. It consists of a 100 m long coiled stainless steel tube, combining ~40 m of 0.25 inch (6.35 mm) tube and ~60 m of 0.125 inch (3.175 mm) tube, along with an automatic shut-off valve and home-made data logger to record temperature and pressure during the flight. A 3 kg meteorological balloon was used to launch the AirCore along with a radiosonde and the payload positioning system. The air is evacuated from the tube during ascent to an altitude of ~30 km due to the pressure difference, while ambient air flushes into the tube as it descends. Upon landing the automatic valve shuts off to

155   prevent any further exchange of the sampled air inside the tube with ambient air. A cavity ring-down spectrometer (CRDS) manufactured by Picarro Inc. is used afterwards to quantify the mole fractions of the target gases (e.g. CO_2 and CH_4) in the AirCore sample.

3 Results and discussions

3.1 Quality of a-priori profiles and their influence on the retrieval results

160   The choice of a-priori VMR vertical profiles for the target gases is important for retrieving correct column abundances from ground-based FTIR spectra. The PROFFAST algorithm for retrieving COCCON observations is a nonlinear least squares

spectral fitting algorithm, scaling an a-priori dry-air mole fraction of profile to generate the best spectral fit to the measured spectrum by using a single scale factor.

In the following section two different sets of a-priori profiles are used for investigating the sensitivity of the retrievals
165 with respect to the choice of the profiles. One set of VMR profiles (MAP) is the one used by TCCON. The profiles are derived from a stand-alone program to generate profiles as described in Toon et al., 2015. These profiles are based on temperature, pressure and humidity generated by National Centers for Environmental Prediction/National Center for Atmospheric Research (NCEP/NCAR), empirically derived from MkIV FTS balloon flights (Toon, 1991) and in-situ GLOBALVIEW data (GLOBALVIEW-CO2, 2006). The MAP profiles are up to 70 km and are sampled on an equidistant 1
170 km grid. Another set of daily profiles (at 12:00 UTC) is provided by CAMS. These daily CAMS profiles have 137 model levels from 0.1 km up to 80 km and the defined corresponding altitudes are based on the 1976 version of the International Civil Aviation Organization (ICAO) Standard Atmosphere.

3.1.1 Comparison of the MAP and the CAMS profiles for the Sodankylä campaign site

The CO_2 and CH_4 profiles of MAP and CAMS in 2017 and 2018 for the Sodankylä campaign site are shown in Figure 1. The
175 left columns show the MAP profiles, the middle columns show the CAMS profiles and the right columns show the difference of the MAP and the CAMS profiles as a function of the altitude. For CO_2 both profiles present similar seasonal changes and the highest near-ground concentration occur in winter and the lowest in summer. However, the CAMS profiles show higher vertical variability and more obvious seasonal changes over the whole year. Most of the time, the MAP profiles show lesser CO_2 concentrations than CAMS as seen in the difference plots for both 2017 and 2018 profiles (Figure 1 right columns). The
180 main differences between MAP and CAMS CO_2 profiles occur in the troposphere and the difference at near ground ranges from -15 ppm to 12 ppm for 2017 and -21 ppm to 12 ppm for 2018, showing a peak-to-peak variability of about 27 ppm in 2017 and 33 ppm in 2018. These differences are mostly negative in the beginning of the year and decrease quickly with time. The difference drops to -14.4 ppm on March 9, then increases up to 11.5 ppm on July 23, 2017, while it is -17.6 ppm on February 7, then increases up to 11.6 ppm August 5, 2018. The MAP profiles become underestimated in autumn and the largest
185 difference at ground level is -14.9 ppm occurring on September 5, 2017 and is -21 ppm on August 9, 2018. In the stratosphere the CAMS CO_2 profiles show smaller vertical changes compared to the MAP profiles over the year, however they are generally higher in concentration than the MAP profiles over 40 km in 2017 and over 30 km in 2018. Altogether, the MAP a-priori profiles agree quite well with the CAMS profiles.

A much larger difference exists in CH_4 between the MAP and the CAMS profiles. CAMS shows a significant seasonal
190 change, especially in the stratosphere, while MAP is more constant and overestimated compared to CAMS over the whole year. In contrast to CO_2, the highest differences between MAP and CAMS appear in the lower stratosphere between 20 km and 40 km as seen for both 2017 and 2018 plots (Figure 1). In the beginning of the year, the difference between MAP and CAMS profiles is around 0.9 ppm at 28 km, and reaches to nearly 1 ppm at a lower level of 20 km in spring. The largest difference reaches up to 1.0 ppm at 22 km on April 12, 2017 and at 20 km on March 12 and 15, 2018. The MAP profiles are

being close to CAMS and the highest difference is around 0.35 ppm at 33 km in summer 2017 and 2018. In winter, the differences are also obvious and near to 0.9 ppm at around 30 km. The steeper vertical gradients together with the dynamical processes occurring in the polar atmosphere make a climatological guess of a-profile shape much harder than for carbon dioxide and therefore the MAP a-priori profiles are less realistic for methane. We will investigate in the next section using AirCore soundings to which degree CAMS is capable of following the actual profile variability.

3.1.2 Comparison of in-situ AirCore profiles and CAMS profiles for the Sodankylä campaign site

The in-situ profiles are derived from the AirCore balloon launches at the Sodankylä campaign site and up to an altitude of approximate 30 km. Figure 2 shows the differences of CO_2 and CH_4 between the AirCore and the CAMS profiles for 10 measurement days in 2017 and 9 measurement days in 2018. The AirCore launches cover the spring to autumn period.

The CAMS CO_2 profiles are generally overestimated compared to the AirCore profiles, with a mean difference on average of 1.35 ppm in 2017 and 3.33 ppm in 2018. In the 10 AirCore launched days in 2017, CAMS profiles are slightly overestimated in the stratosphere, while the tropospheric CAMS profiles are closer to the AirCore profiles in summer than those in autumn 2017. Two peak differences are found at altitude around 9 km with -5.98 ppm (AirCore - CAMS) on April 24 and -9.46 ppm on April 26 and another peak at around 1 km with -5.76 ppm on September 5, 2017. The CAMS profiles show a slightly higher overestimation in CO_2 profiles in summer than another days in 2018 and which is likely due to the seasonal bias in CAMS. In general, CAMS profiles are overestimated over the whole vertical altitude range and differences in the stratospheric part are quite constant throughout the year. The averaged difference over 10 km is about -1.7 ppm in 2017 and -2.9 ppm in 2018.

The significant differences for CH_4 in the stratosphere can be seen in the early year when comparing CAMS with in-situ AirCore profiles. Two obvious differences occur on April 21 and 26, whose plots are highlight with additional red and green dots in the right corner of Figure 2. CAMS underestimates 0.16 ppm atmospheric CH_4 abundances at around 19 km on April 21, 2017 and overestimates approximately 0.34 ppm CH_4 at around 22 km on April 26, 2017. The significant stratospheric subsidence in April 2017 is probably caused by the polar vortex. Figure 3 (first row) shows N_2O data from the Microwave Limb Sounder (MLS) on the Aura satellite for three days in April and one day in May 2017 when AirCore flights were performed. Because of its long life time, N_2O is a good tracer for estimating the position of the polar vortex. Therefore, N_2O concentrations at the 46 hPa level, approximately at the height of 20 km, is used here to study the XCH_4 abnormal observations. Obvious stratospheric subsidence is clearly seen over Finland in April and disappeared in May 2017. For the CH_4 profiles in the troposphere CAMS profiles are slightly underestimated in spring and overestimated in summer 2017 as compared to AirCore, while the CAMS CH_4 profile is close to AirCore from approximately 3 km up to 12 km, coupled with an underestimated profile in the stratosphere on October 9, 2017. The tropospheric CAMS profiles for 2018 are very similar to the AirCore profiles for all measurement days. However, the CAMS profile on April 17, 2018 have three obvious peaks with underestimations of 0.21 ppm at 20 km and of 0.32 ppm at 22 km and an overestimation of 0.23 ppm at 21 km. The CAMS overestimates the CH_4 concentration in the lower stratosphere on October 3, 2018. The difference between CAMS and AirCore

profiles increases with height and reaches up to 0.13 ppm at 21 km, however, CAMS show an underestimation at higher levels, with a peak value of 0.15 ppm at 27 km.

Despite the remaining discrepancies, CAMS CH_4 profiles approximate the true state of the polar atmosphere considerably
230   better than the MAP profiles used as a-priori for TCCON.

3.1.3 Comparison of COCCON and TCCON datasets with different a-priori profiles

When directly comparing the measurements of different remote sounders, it is necessary to account for differing observing systems characteristics, particularly the a-priori profiles used and the different sensitivity characteristic (Rodgers and Connor, 2003). In the following, we discuss the impact of the a-priori profile choice.

235   Figure 4 shows the comparison of XCO_2 and XCH_4 between COCCON and co-located TCCON as a reference in Sodankylä in 2017 and 2018. Since the same a-priori profiles are used, the differences between these two datasets are mainly from the different smoothing error characteristics. The partial column sensitivities of TCCON and COCCON both are imperfect and differ from each other, the kernels are shown in Figure 5 in the work by Hedelius et al. (2017). Therefore we expect that a more realistic a-priori profile will bring the results in better agreement. The left panel of Figure 4 shows results generated with
240   the MAP a-priori profiles, while the right panel show the results achieved with the CAMS a-priori profiles. The coincident data points are based on a 10-minute average and the error bars are presented with standard errors. Processed with the MAP profiles, COCCON and TCCON data show a generally good agreement in both XCO_2 and XCH_4. The COCCON instrument measures 0.74 ppm (±0.49 ppm) lower XCO_2 and 0.17 ppb (±3.77 ppb) lower XCH_4 on average than TCCON retrievals in 2017. The XCO_2 difference between COCCON and TCCON is slightly reduced in 2018, when COCCON retrievals are 0.57
245   ppm (± 0.49 ppm) lower in XCO_2. The difference of XCH_4 between COCCON and TCCON triples in 2018 compared to that of the previous year, when COCCON measures 0.57 ppb (± 3.47 ppb) lower amount of XCH_4. One reason for the change of XCH_4 is because the obvious biases in April 2017 which increases the yearly averaged value of the COCCON XCH_4.

When using CAMS profiles as the a-priori information, COCCON data show better correlations with TCCON data than using MAP a-priori profiles, especially in XCH_4. This is mainly because CAMS profiles have better seasonal variations,
250   especially for CH_4. A significant bias of XCH_4 in April 2017 and in March 2018 were found when using MAP a-priori profiles, which is mainly caused by the polar vortex (see Figure 3). The stratospheric subsidence was not included in the MAP profiles, resulting in high biases. However, these biases disappeared in the data comparison when using CAMS profiles and the correlation improved due to the better modeled profile information from CAMS. Ostler et al. (2014) investigated the stratospheric subsidence caused by the influence of the polar vortex and found different impacts on mid-infrared and near-
255   infrared retrievals because of the differing sensitivity depending on the altitude, although the same a-priori VMR profiles were used. Here, a similar mechanism is at work, the different sensitivities between TCCON and COCCON generate different smoothing errors. The more realistic CAMS a-priori information reduces these discrepancies. The COCCON data discussed below are using the CAMS profiles as a-prior profiles.

3.2 Comparing COCCON observations with CAMS and S5P

260 ### 3.2.1 XCO_2

The XCO_2 intercomparison between CAMS and COCCON retrievals at Kiruna (left) and Sodankylä (right) sites from 2017 to 2019 are shown in Figure 5. COCCON retrievals show a good and similar agreement with CAMS data at both sites with R^2 values of 0.9530 in Kiruna and 0.9756 in Sodankylä. The CAMS data are biased high in comparison to COCCON with a mean bias of 3.72 ppm and a standard deviation of 1.80 ppm in Kiruna and with a mean bias of 3.46 ppm and a standard deviation

265 of 1.73 ppm in Sodankylä. The increase of bias as a function of time is related to the CAMS model overestimation and is also reported by Christophe et al., 2019. The Orbiting Carbon Observatory 2 (OCO-2) satellite also provides global coverage of CO_2 observations. The CO_2 comparison between the OCO-2 satellite and the COCCON would be another subject of the future work and is not shown here.

3.2.2 XCH_4

270 The correlation of XCH_4 between CAMS and COCCON measurements is more scattered than that of XCO_2 (see Figure 6, upper panel). The R^2 value decreased by nearly one third to 0.6236 in Kiruna and nearly half to 0.5292 in Sodankylä. CAMS data on average are biased high by about 0.33 ppb (±11.93 ppb) in Kiruna, and 7.39 ppb (±10.92 ppb) in Sodankylä. The most significantly high bias occur at both sites from March 2017 to June 2017. Though CAMS profiles show better seasonal variability in CH_4 than the MAP profiles, they are still not perfect compared to the realistic profiles, especially during a period

275 of strong stratospheric subsidence (see Figure 2, compared with AirCore profiles). These imperfect profile shapes of CAMS probably result in the high bias in March and April. The highest differences are found in June 2017 with 23.06 ppb in Kiruna and 29.42 ppb in Sodankylä. However, the much higher bias in June is more likely due to the bias from CAMS itself (as reported in Christophe et al., 2019), and is not found when comparing COCCON and TCCON measurements for 2017. This is because the hydroxyl radical (OH) is the primary CH_4 sink in the troposphere via oxidization (Lelieveld et al., 2016; Rigby

280 et al., 2017) and its amount is generally higher in summer. Wang et al. (2019) evaluated the CAMS trace gases using aircraft observations and found an underestimation of OH concentrations in the Arctic. The underestimated concentrations of OH weakens the loss of CH_4 concentration in the CAMS model, which contribute to a higher amount of CH_4. There is a different situation found in August 2018, when COCCON measures 14.33 ppb higher XCH_4 at Kiruna site and 4.54 ppb higher at Sodankylä site. Table 1 shows the monthly averaged difference of XCH_4 between CAMS and COCCON at both sites in 2017

285 and 2018.

The comparison between S5P and COCCON measurements shows a different situation, where the S5P satellite generally measures lower atmospheric XCH_4 than COCCON. However, obvious biases are found in March and April 2019 (presenting in yellow color), when S5P measured higher XCH_4. Excluding these two months measurements, S5P measures 9.69 ppb (±20.51 ppb) lower XCH_4 in Kiruna and 3.36 ppb (±17.05 ppb) lower in Sodankylä. Compared to the correlation between

290 CAMS and COCCON retrievals, the correlation between S5P and COCCON measurements is poorer and the values of R^2 are

nearly halved, with 0.2947 at the Kiruna site and 0.2909 at Sodankylä site. The error bar represents the standard error of mean, caused by higher standard deviation or/and lesser number of observations. Higher error bars are found at Kiruna site and this might be due to the more complex terrain at the Kiruna site where mountains are located to the west of Kiruna. For testing the resulting effects, we shifted the center of the coincidence area 50 km to the east to reduce the effects of mountains, but the

295   higher scatters largely remains. This is further investigated by comparing the ground pressure derived from S5P to the values used by COCCON. The altitude measured by S5P satellite ranges approximately from 220 m to 960 m in the defined area around Kiruna, while it ranges only from 118 m to 358 m in Sodankylä area. When we interpolate the S5P pressure at the two sites to the altitude of two COCCON locations separately, the correlations at both sites show good agreement when the R^2 is 0.9960 at Kiruna and 0.9894 at Sodankylä (see Figure 7).

300   **3.2.3 Effects of albedo and viewing zenith angle on XCH4**

The officially released S5P data also contains other parameters, like albedo retrieved in the same SWIR region and viewing zenith angle (VZA). The sensitivities of the ratio of XCH4 (S5P measurements divided by COCCON) to albedo and VZA at each site are presented in Figure 8. The albedo ranges from 0.03 to 0.10 in the period of May 2018 – September 2019, showing no obvious effects on the ratio of XCH4. Both sites show similar situation with the average ratio of 0.9949 ± 0.0118 in Kiruna

305   and 0.9953 ± 0.0089 in Sodankylä. The VZA of S5P satellite changes approximately from 2° to 60° in the available time period. The sensitivity analysis shows that there are negligible changes in measuring XCH4 when VZA changes.

3.4 Comparison of gradients measurement at two sites between CAMS/S5P and COCCON

To study the capability to measure the gradients of XCO2 (ΔXCO2) and XCH4 (ΔXCH4) on reginal scales of both S5P and COCCON, the differences of XCO2 and XCH4 with respect to CAMS between Kiruna and Sodankylä are presented in Figure

310   9 and Figure 10. As S5P does not measure CO2, the ΔXCO2 results are shown only for CAMS vs COCCON.

The ΔXCO2 comparison between CAMS and COCCON show a much poorer correlation (R^2 = 0.3322) than the comparison of XCO2 between two sites (R^2 = 0.9643, mean value of both sites over the whole measurements), as to be expected: the ΔXCO2 signals are very small (on the order of 0.5 ppm). Still, a positive correlation in ΔXCO2 and similar amplitudes are found in CAMS and COCCON data. If the comparison would be dominated either by horizontal smoothing effects due to the

315   limited resolution of the model (would reduce the spread along the y-axis of Figure 10 or by the uncertainties of the COCCON measurement (would amplify the spread along the x-axis of Figure 10, the variability ranges would differ significantly.

For ΔXCH4 the comparison between CAMS and COCCON measurements (Figure 10 left panel) shows a better correlation (R^2 = 0.4117) than that between S5P and COCCON (Figure 10 right panel). S5P results show higher scattering, resulting in a poorer correlation (R^2 = 0.2078) with COCCON. This nearly half difference is probably due to the smaller number of the

320   coincident measurements between S5P and COCCON. There are only 50 coincident measurements between S5P and COCCON in total, covering 17 days in 2018 and 16 days in 2019, while there are 86 coincident measurements between CAMS and COCCON in total, covering 17 days in 2017, 29 days in 2018 and 26 days in 2019. Figure 10, middle panel shows the

agreement between CAMS and COCCON for the subset of days with S5P observations. The correlation in the restricted days is similar to the correlation between S5P and COCCON. CAMS, COCCON and S5P seem to be able to detect methane
325   gradients on regional scales. Table A. 1 lists the statistics of S5P data coincident with COCCON data when S5P overpasses both sites in one day.

4 Conclusions

In this study, two COCCON instruments are used to perform multi-year measurements at Kiruna and Sodankylä. The instruments demonstrate useful performance for accuracy, measuring gradients of column-averaged greenhouse gas
330   abundances on regional scales. We first compared the profiles derived from CAMS with the TCCON official profiles (MAP). For CO_2 vertical profiles, both CAMS and MAP present similar seasonal variations, though CAMS profiles show higher vertical variability and more obvious seasonal changes over the whole time period of analysis. The main differences between them dominate in the troposphere, with peak-to-peak variability of about 25 ppm. However, the CH_4 profiles derived from CAMS show a significant seasonal change, especially in the stratosphere, while MAP is more constant and overestimated over
335   the whole year. The CH_4 difference reaches up to 1 ppm at around 25 km height in April 2018. The AirCore balloon launches were performed as an auxiliary activity during the Finland campaign. CAMS profiles show a better agreement with the in-situ measurements derived from AirCore launches than the official TCCON MAP a-priori profiles. Especially, CAMS presents better profiles for CH_4 in April, while the MAP profiles do not show the stratospheric subsidence caused by the polar vortex.

MAP and CAMS profiles are used as apriori information in processing COCCON and TCCON data at the Sodankylä and
340   Kiruna sites. The correlation between COCCON and TCCON data improved for both XCO_2 and XCH_4 when using CAMS a-priori profiles. R^2 increased to 0.9925 in 2017 and 0.9863 in 2018 for XCO_2 and 0.9708 in 2017 and 0.9635 in 2018 for XCH_4. The obvious biases in April 2017 when comparing COCCON to the TCCON data (using MAP profiles) is mainly caused by the polar vortex. However, these outliers disappeared in the data comparison when data are processed with CAMS profiles. Different instrument show different sensitivity to the a-priori profiles and the CAMS profiles might be a good choice to
345   improve the data accuracy.

We also compared XCO_2 and XCH_4 between COCCON and CAMS and XCH_4 between COCCON and the S5P satellite in Kiruna and Sodankylä. The XCO_2 comparisons between COCCON and CAMS at both sites show similar and good agreement with a mean bias of 3.72 ppm, standard deviation of 1.80 ppm, and R^2 of 0.9530 in Kiruna; with a mean bias of 3.46 ppm, standard deviation of 1.73 ppm, and R^2 of 0.9756 in Sodankylä. The correlations of XCH_4 between COCCON and CAMS are
350   relatively poorer than the XCO_2 correlations with R^2 of 0.6236 in Kiruna and 0.4673 in Sodankylä. CAMS mostly overestimated XCH_4 in comparison to COCCON (approximately 0.33 ppb (±11.93 ppb) higher XCH_4 in Kiruna, and 7.39 ppb (±10.92 ppb) higher XCH_4 in Sodankylä). In contrast, the S5P satellite generally measures lower atmospheric XCH_4 than COCCON, with a mean bias of 9.69 ppb, standard deviation of 20.51 ppb and R^2 of 0.2947 in Kiruna; a mean bias of 3.36 ppb,

standard deviation of 17.05 ppb and R^2 of 0.2909 in Sodankylä. In addition, no obvious variability is found when albedo and

355   viewing zenith angle of S5P changes.

When studying the possibility of measuring gradients of XCO_2 and XCH_4 for the region between Kiruna and Sodankylä, we compared the COCCON results with CAMS and S5P (only for XCH_4). For ΔXCO_2 CAMS show higher values and has a R^2 value of 0.3322. For ΔXCH_4 COCCON shows a better correlation with the CAMS (slope = 0.6482, R^2 = 0.4117) than with the S5P (slope = 0.5791, R^2 = 0.2078). When limiting the COCCON and CAMS data to the S5P overpass days, the correlation

360   of ΔXCH_4 between them decreased (slope = 0.5304, R^2 = 0.2242) and is close to the correlation between S5P and COCCON. The lower correlation between COCCON and S5P results is probably due to the smaller dataset. COCCON observations can be used for the quantification of sources and sinks of greenhouse gases and for the validation of space borne observations.

365   *Data availability*. The data is accessible by contacting the corresponding author (qiansi.tu@kit.edu).

Table 1. Monthly averaged difference of XCH$_4$ between CAMS and COCCON at two sites in 2017 and 2018.

	Kiruna		Sodankylä	
	2017	2018	2017	2018
February	--	-10.60 ± 0.0	--	--
March	-6.75 ± 7.18	-6.85 ± 6.60	-10.43 ± 3.58	-7.88 ± 4.56
April	-8.37 ± 5.46	-0.63 ± 3.90	-12.20 ± 5.01	-5.42 ± 4.60
May	-11.02 ± 5.10	-3.12 ± 5.81	-19.53 ± 6.47	-6.12 ± 6.47
June	-23.06 ± 8.98	-4.40 ± 4.63	-29.42 ± 6.81	-6.63 ± 4.00
July	--	-4.71 ± 7.68	-10.66 ± 9.86	-9.22 ± 7.97
August	-0.15 ± 1.31	14.33 ± 3.35	-5.62 ± 4.48	4.54 ± 10.02
September	3.22 ± 6.06	6.45 ± 3.57	-3.13 ± 7.86	-0.79 ± 0.29

370
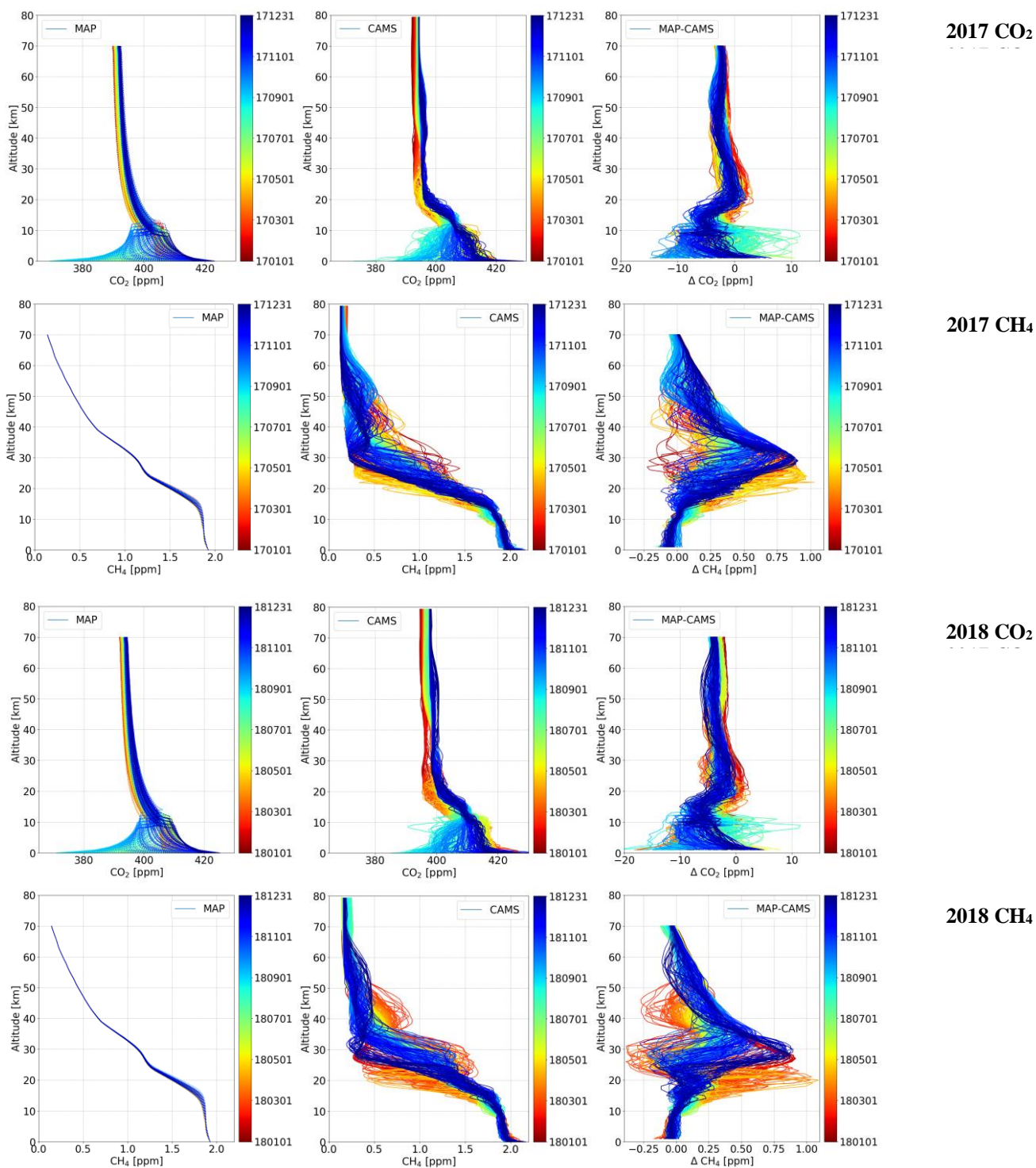
Figure 1. Profiles of MAP (left columns), CAMS (middle columns) and the difference of MAP-CAMS (right columns) for CO_2 and CH_4 in 2017 and 2018.
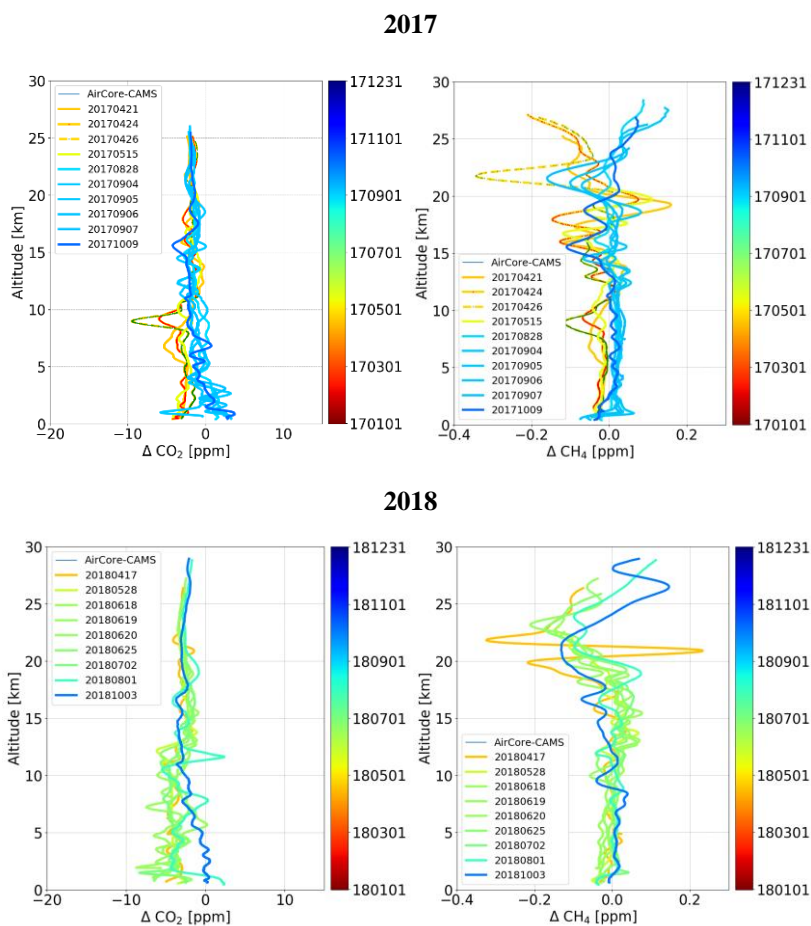
Figure 2. Differences between AirCore and CAMS for CO_2 (left) and CH_4 (right) profiles in 2017 and 2018.

380
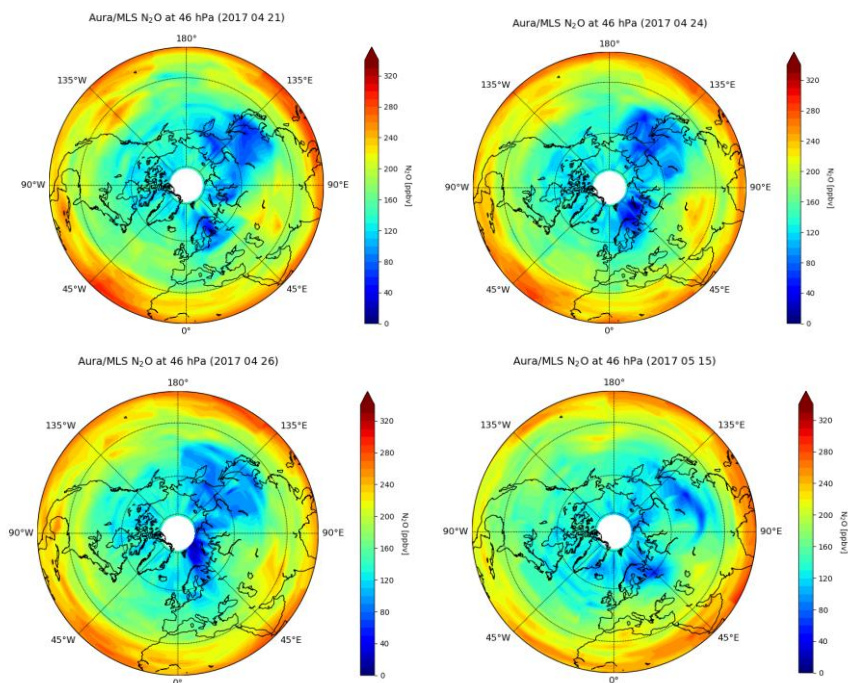
2017

385
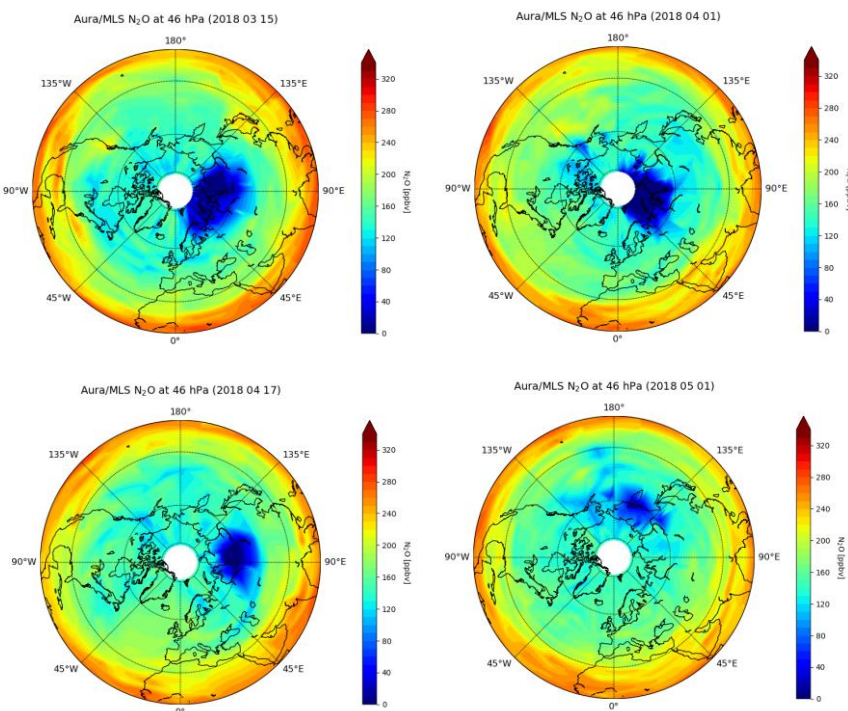
2018

Figure 3. Polar vortex in north hemisphere in four days in April – May 2017 and four days in March – May 2018.
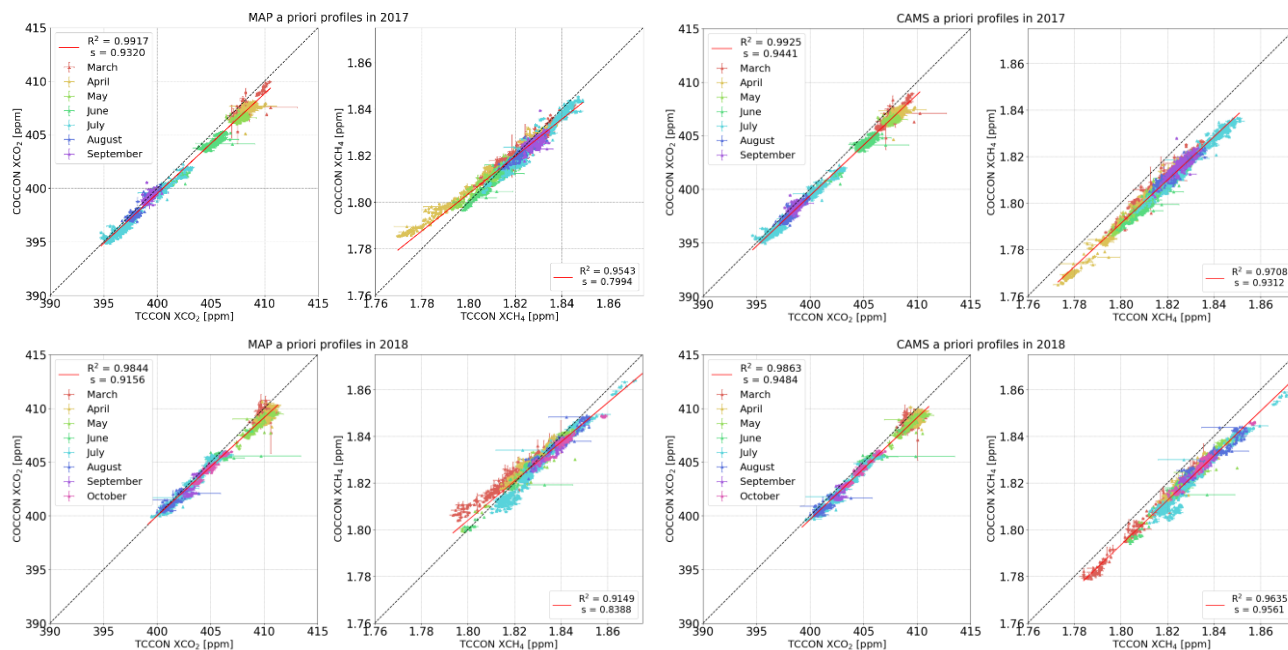
Figure 4. Comparisons of COCCON and TCCON data in 2017 and 2018 with using MAP (left) and CAMS (right) profiles as prior profiles. The slope of the relationship is represented by "s" in the figure, and the coefficient of determination is represented by "R^2". Each point represents a 10-minute average of coincident between COCCON and TCCON measurements. The red line represents the best fit line and the black line is the one-to-one line.
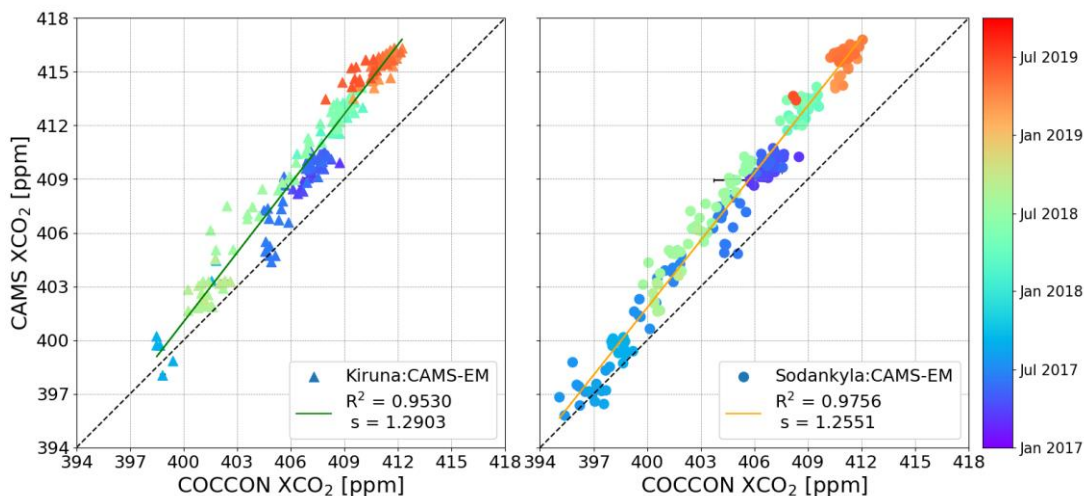
Figure 5. XCO_2 comparison between CAMS and COCCON in Kiruna (left) and Sodankylä (right). Every point represents hourly average value of coincident CAMS and COCCON measurements. The annotations follow those in Figure 4.

400
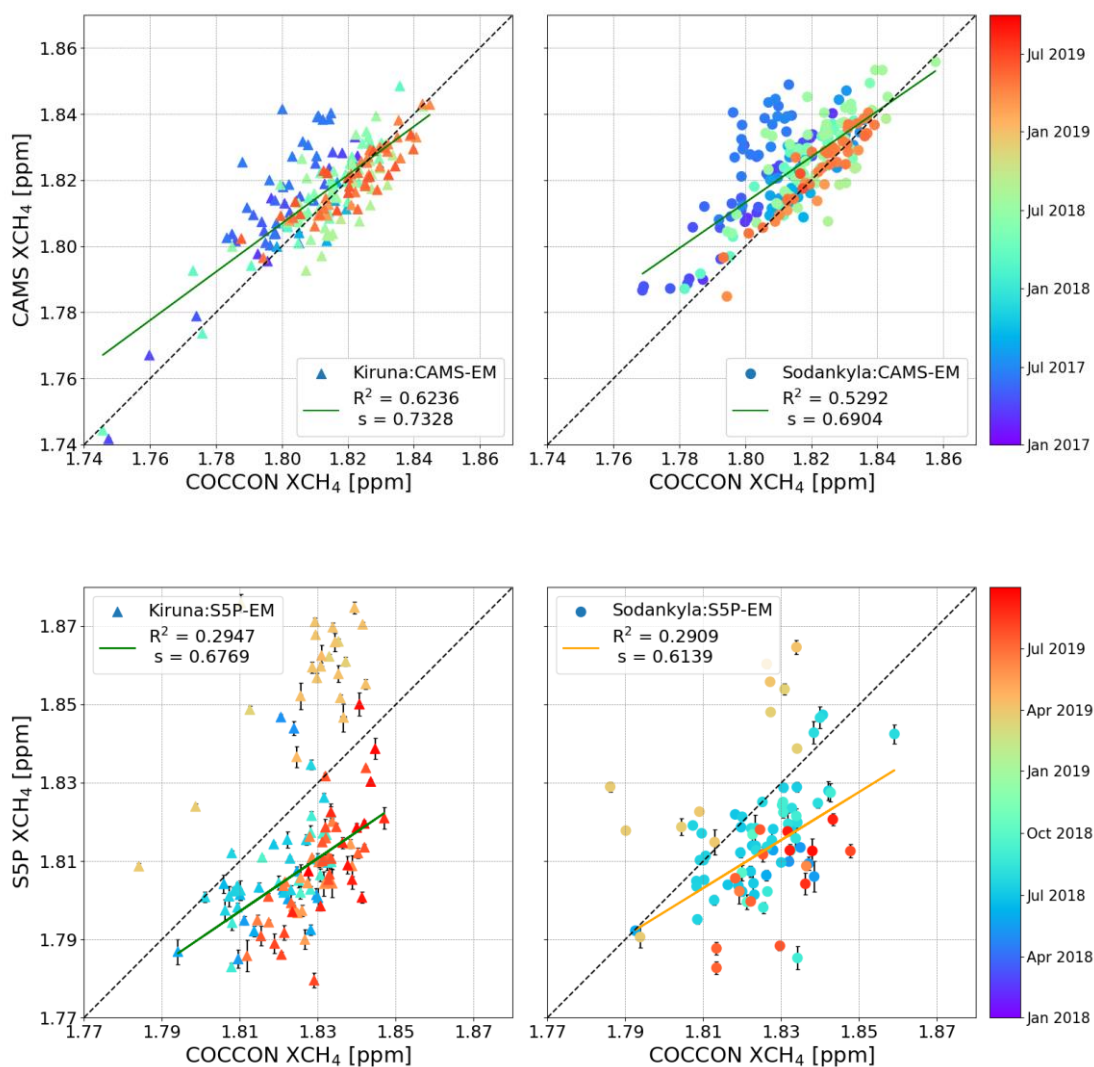
Figure 6. XCH4 comparison between CAMS (top panel) or S5P (lower panel) and COCCON in Kiruna (left) and Sodankylä (right). Every point represents coincident CAMS and COCCON measurements. The annotations follow those in Figure 4. Note that the fitting line derived from the data exclude the March and April, 2019. It is noted that the color bar starts from 2018 rather than 2017 for better distinguishing data.

405

410
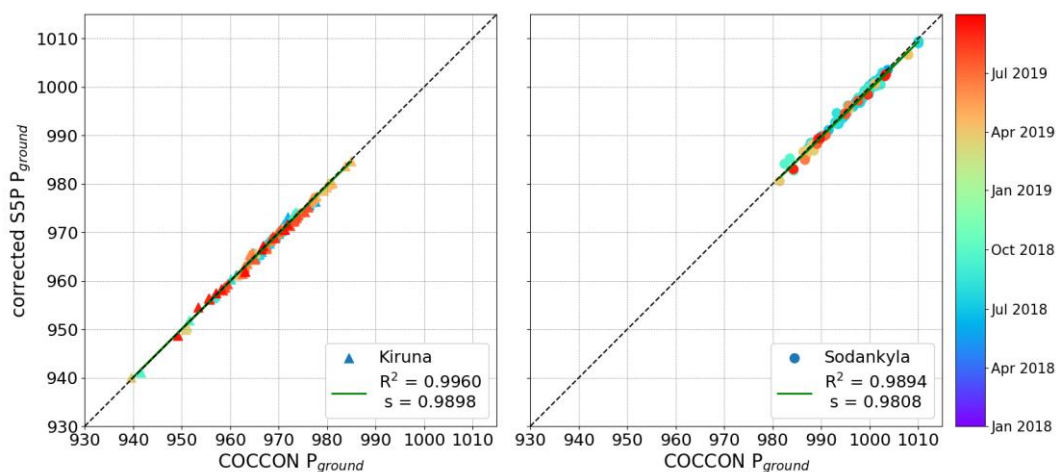
Figure 7. Ground pressure comparison between S5P and COCCON in Kiruna (left) and Sodankylä (right). The S5P pressure is interpolated to the height of COCCON. Every point represents coincident S5P and COCCON measurements. The annotations follow those in Figure 4. It is noted that the color bar starts from 2018 rather than 2017 for better distinguishing data.
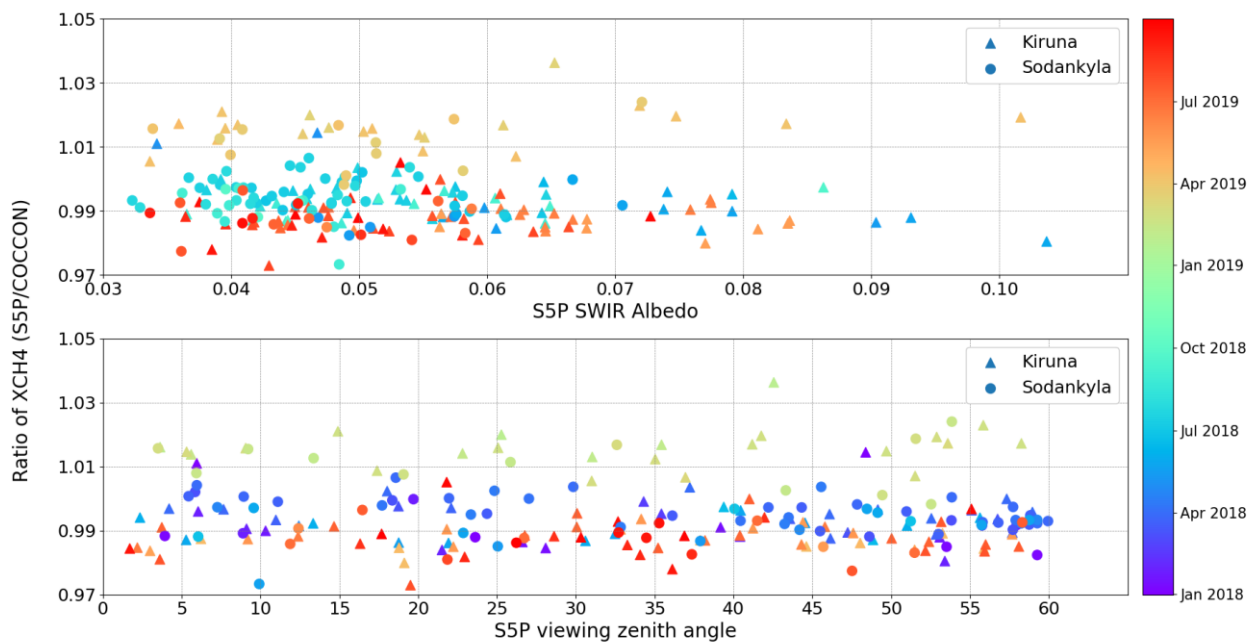
Figure 8. The ratio of XCH4 (S5P divided by COCCON results) at two different sites as a function of albedo (top) and viewing zenith angle (bottom) from S5P. It is noted that the color bar starts from 2018 rather than 2017 for better distinguishing data.
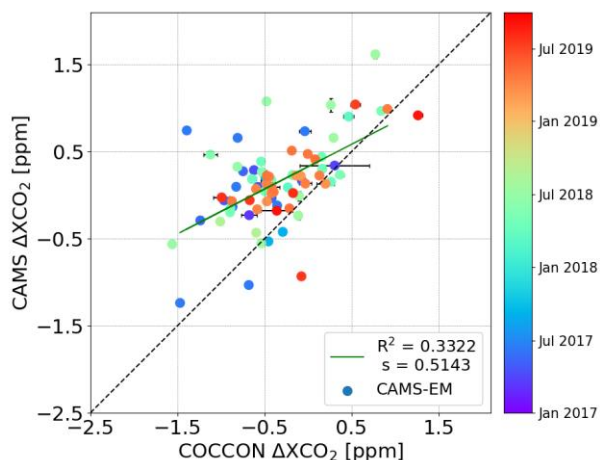
Figure 9. Difference of XCO_2 measured between Kiruna and Sodankylä. Plot showing the comparison between CAMS and COCCON. The annotations follow those in Figure 4.
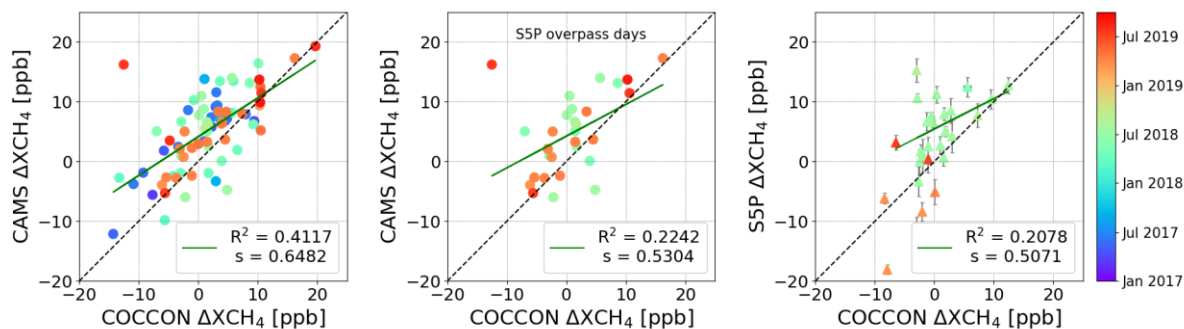
Figure 10. Difference of XCH_4 measured between Kiruna and Sodankylä. Left panel: plot showing the comparison between CAMS and COCCON. Middle panel: plot showing the comparison between CAMS and COCCON during the S5P overpass days. Right panel: plot showing the comparison between S5P and COCCON. The annotations follow those in Figure 4.

Appendix

Table A. 1 the statistics of S5P data coincident with COCCON data when S5P overpasses both sites in one day.

Overpass date	Overpass time	Kiruna		Sodankylä	
		measurements Nr.	Error	measurements Nr.	Error
2018-05-11	09:46	1	--	30	9.5631E-4
2018-05-25	12:04	2	0.00129	1	9.7769E-4
2018-05-29	10:48	11	0.00319	44	9.3367E-4
2018-05-31	10:10	21	0.00236	19	0.0014
2018-07-02	08:31	58	0.00113	110	8.44187E-4
	10:10	243	5.48425E-4	404	3.25961E-4
	11:51	89	9.28037E-4	112	6.38277E-4
2018-07-10	09:21	56	0.00134	190	5.23952E-4
2018-07-12	08:43	29	0.00211	61	0.00126
	10:23	200	5.9486E-4	310	4.79266E-4
	12:04	55	0.00105	27	9.43214E-4
2018-07-13	08:25	27	0.00152	16	0.00144
	10:04	72	0.00113	41	0.00111
	11:45	6	0.00195	4	6.71639E-4
2018-07-16	09:08	14	0.00256	115	8.18677E-4
	10:48	76	9.76244E-4	228	4.38376E-4
2018-07-17	08:50	58	0.00118	92	9.55501E-4
	10:29	85	8.76049E-4	325	4.04797E-4
2018-07-18	08:31	31	0.00132	92	9.66493E-4
	10:11	112	7.06507E-4	267	5.33282E-4
	11:51	8	0.0028	16	0.00116
2018-07-19	08:13	17	0.00256	70	8.93628E-4
	09:52	6	0.00299	386	3.26368E-4
2018-07-20	09:33	40	0.00131	280	4.6468E-4
2018-07-27	09:02	1	--	107	8.6095E-4
2018-08-08	10:17	13	0.00179	2	0.00338
2018-08-31	09:46	27	0.00177	121	9.12589E-4
	11:26	8	0.00249	7	0.00172

2018-09-03	10:30	32	0.00172	143	9.18697E-4
2019-03-19	10:36	231	0.00060	24	0.00146
2019-03-22	09:40	182	0.00070	452	0.00041
	11:20	85	0.0012	229	0.00748
2019-03-26	10:05	283	0.00067	430	0.00060
2019-04-05	08:38	82	0.00101	139	0.00104
	10:17	358	0.00060	468	0.00052
2019-04-05	11:58	106	0.00114	1	--
2019-04-08	09:21	38	0.00120	21	0.00170
2019-04-10	12:04	56	0.00125	1	--
2019-04-14	09:09	16	0.00542	1	--
	10:49	22	0.00339	1	--
2019-04-15	08:50	59	0.00269	1	--
2019-04-16	08:31	1	--	1	--
	10:11	4	0.00504	1	--
2019-04-18	09:34	26	0.00267	1	--
	11:14	3	0.01216	1	--
2019-04-26	10:23	2	0.00477	1	--
2019-06-07	08:56	4	0.00351	81	0.00102
2019-07-12	09:39	6	0.00212	191	0.00063
2019-07-22	09:52	56	0.00097	125	0.00076
2019-07-25	12:16	2	0.00487	1	--
2019-09-19	09:46	2	0.00067	2	0.00309

435

Author contributions. Frank Hase, Thomas Blumenstock and Qiansi Tu developed the research question. Qiansi Tu wrote the manuscript and performed the data analysis with support from Frank Hase, Thomas Blumenstock and Mahesh Kumar Sha.

440   Qiansi Tu, Thomas Blumenstock, Pauli Heikkinen, Rigel Kivi and Uwe Raffalski took an active part in the field campaign by operating the COCCON spectrometers and collecting data. Rigel Kivi and Pauli Heikkinen also operate the TCCON station at Sodankylä site and provided data. Jochen Landgraf, Alba Lorente and Tobias Borsdorff offered technical support in analyzing S5P satellite data. Huilin Chen provided the AirCore data. All authors discussed the results and contributed to the final manuscript.

445

Competing interests. The authors declare that they have no conflict of interest.

450   *Acknowledgements.*

We thank Xiaobo Yang in the Copernicus User Support Team at ECMWF providing the CAMS model data, which were generated using Copernicus Atmosphere Monitoring Service (2017 - 2019) information. We would like to thank MLS team for providing the N_2O data and Farahnaz Khosrawi for producing the N_2O figures. The work presented here overlaps with the Fiducial Reference Measurements for Ground-Based Infrared Greenhouse Gas Observations (FRM4GHG) project funded by

455   European Space Agency under the grant agreement number
ESA-IPL-POE-LG-cl-LE-2015-1129. The AirCore launches are partly supported by the EU RINGO project.

The article processing charges for this open-access publication were covered by a Research Centre of the Helmholtz

460   Association.

References

Apituley, A., Pedergnana, M., Sneep, M., Veefkind, J.P., Loyola, D. and Hasekamp, O.: Sentinel-5 precursor/TROPOMI Level 2 Product User Manual Methane, source: SRON/KNMI, ref: SRON-S5P-LEV2-MA-001, issue: 0.11.6, date: 2017-06-24.

Bovensmann, Heinrich & Burrows, John & Buchwitz, M. & Frerick, Johannes & Noel, Suresh & Rozanov, V. & Chance, & Kelly, & Goede, A.. (1999). SCIAMACHY: mission objectives and measurement modes. J. Atmos. Sci.. 56. 10.1175/1520-0469(1999)056<0127:SMOAMM>2.0.CO;2.

Butz, A., Galli, A., Hasekamp, O., Landgraf, J., Tol, P., and Aben, I.: TROPOMI aboard Sentinel-5 Precursor: Prospective performance of CH4 retrievals for aerosol and cirrus loaded atmospheres, Remote Sens. Environ., 120, 267–276, https://doi.org/10.1016/j.rse.2011.05.030, 2012.

Butz, A., Dinger, A. S., Bobrowski, N., Kostinek, J., Fieber, L., Fischerkeller, C., Giuffrida, G. B., Hase, F., Klappenbach, F., Kuhn, J., Lübcke, P., Tirpitz, L., and Tu, Q.: Remote sensing of volcanic CO2, HF, HCl, SO2, and BrO in the downwind plume of Mt. Etna, Atmos. Meas. Tech., 10, 1–14, https://doi.org/10.5194/amt-10-1-2017, 2017.

Christophe, Y., M. Ramonet, A. Wagner, M. Schulz, H. J. Eskes, S. Basart, A. Benedictow, Y. Bennouna, A.-M. Blechschmidt, S. Chabrillat, E. Cuevas, A. El-Yazidi, H. Flentje, K.M. Hansen, U. Im, J. Kapsomenakis, B. Langerock, A. Richter, N. Sudarchikova, V. Thouret, T. Warneke, C. Zerefos, Validation report of the CAMS near-real-time global atmospheric composition service: Period March - May 2019, Copernicus Atmosphere Monitoring Service (CAMS) report, CAMS84_2018SC1_D1.1.1_MAM2019_v1.pdf, September 2019, doi:10.24380/1t4q-1h53, 2019.

Frey, M., Hase, F., Blumenstock, T., Groß, J., Kiel, M., Mengistu Tsidu, G., Schäfer, K., Sha, K. M., and Orphal, J.: Calibration and instrumental line shape characterization of a set of portable FTIR spectrometers for detecting greenhouse gas emissions, Atmos. Meas. Tech., 8, 3047–3057, doi:10.5194/amt-8-3047-2015, 2015.

Frey, M., Sha, M. K., Hase, F., Kiel, M., Blumenstock, T., Harig, R., Surawicz, G., Deutscher, N. M., Shiomi, K., Franklin, J. E., Bösch, H., Chen, J., Grutter, M., Ohyama, H., Sun, Y., Butz, A., Mengistu Tsidu, G., Ene, D., Wunch, D., Cao, Z., Garcia, O., Ramonet, M., Vogel, F., and Orphal, J.: Building the COllaborative Carbon Column Observing Network (COCCON): long-term stability and ensemble performance of the EM27/SUN Fourier transform spectrometer, Atmos. Meas. Tech., 12, 1513–1530, https://doi.org/10.5194/amt-12-1513-2019, 2019.

Gisi, M., Hase, F., Dohe, S., Blumenstock, T., Simon, A., and Keens, A.: XCO2-measurements with a tabletop FTS using solar absorption spectroscopy, Atmos. Meas. Tech., 5, 2969–2980, doi:10.5194/amt-5-2969-2012, 2012.

GLOBALVIEW-CO2: Cooperative Atmospheric Data Integration Project – Carbon Dioxide, CD-ROM, NOAA GMD, Boulder, Colorado, 2006.

Hase, F., Blumenstock, T., and Paton-Walsh, C.: Analysis of the instrumental line shape of high-resolution fourier transform IR spectrometers with gas cell measurements and new retrieval software., Appl. Opt., 38, 3417–3422, doi:10.1364/AO.38.003417, 1999.

Hedelius, J. K., Parker, H., Wunch, D., Roehl, C. M., Viatte, C., Newman, S., Toon, G. C., Podolske, J. R., Hillyard, P. W., Iraci, L. T., Dubey, M. K., and Wennberg, P. O.: Intercomparability of X_{CO2} and X_{CH4} from the United States TCCON sites, Atmos. Meas. Tech., 10, 1481–1493, https://doi.org/10.5194/amt-10-1481-2017, 2017.

Hu, H., Landgraf, J., Detmers, R., Borsdorff, T., Brugh, J. A. d., Aben, I., Butz, A., and Hasekamp, O.: Toward Global Mapping of Methane With TROPOMI: First Results and Intersatellite Comparison to GOSAT, Geophys. Res. Lett., 45, 3682–3689, https://doi.org/10.1002/2018GL077259, 2018.

Inness, A., Ades, M., Agusti-Panareda, A., Barre, J., Benedictow, A., Blechschmidt, A.-M., Dominguez, J., Engelen, R. J., Eskes, H., Flemming, J., Huijnen, V., Jones, L., Kipling, Z., Massart, S., Parrington, M., Peuch, V.-H., Razinger, M., Remy, S., Schulz, M, and Suttie, M.: The CAMS reanalysis of atmospheric composition, Atmos. Chem. Phys., 19, 3515–3556, https://doi.org/10.5194/acp-19-3515-2019, 2019.

IPCC, 2013: Climate Change 2013: The Physical Science Basis. Contribution of Working Group I to the Fifth Assessment Report of the Intergovernmental Panel on Climate Change [Stocker, T.F., D. Qin, G.-K. Plattner, M. Tignor, S.K. Allen, J. Boschung, A. Nauels, Y. Xia, V. Bex and P.M. Midgley (eds.)]. Cambridge University Press, Cambridge, United Kingdom and New York, NY, USA, 1535 pp.

Karion, A., Sweeney, C., Tans, P., and Newberger, T.: Air-Core: An Innovative Atmospheric Sampling System, Journal of Atmospheric and Oceanic Technology, 27, 1839–1853, 40 https://doi.org/10.1175/2010JTECHA1448.1, https://doi.org/10.1175/2010JTECHA1448.1, 2010.

Kille, N., Chiu, R., Frey, M., Hase, F., Sha, M. K., Blumenstock, T., Hannigan, J. W., Orphal, J., Bon, D. and Voklamer, R.: Separation of methane emissions from agricultural and natural gas sources in the Colorado Front Range. Geophysical Research Letters, 46, 3990– 3998. https://doi.org/10.1029/2019GL082132, 2019.

Kivi, R. and Heikkinen, P.: Fourier transform spectrometer measurements of column CO_2 at Sodankylä, Finland, Geosci. Instrum. Method. Data Syst., 5, 271–279, https://doi.org/10.5194/gi-5-271-2016, 2016.

Klappenbach, F., Bertleff, M., Kostinek, J., Hase, F., Blumenstock, T., Agusti-Panareda, A., Razinger, M., and Butz, A.: Accurate mobile remote sensing of XCO2 and XCH4 latitudinal transects from aboard a research vessel, Atmos. Meas. Tech., 8, 5023–5038, doi:10.5194/amt-8-5023-2015, 2015.

Lambert, J.-C., A. Keppens, D. Hubert, B. Langerock, K.-U. Eichmann, Q. Kleipool, M. Sneep, T. Verhoelst, T. Wagner, M. Weber, C. Ahn, A. Argyrouli, D. Balis, K.L. Chan, S. Compernolle, M. de Graaf, I. De Smedt, H. Eskes, A.M. Fjæraa, K. Garane, J.F. Gleason, F. Goutail, J. Granville, P. Hedelt, K.-P. Heue, G. Jaross, ML. Koukouli, J. Landgraf, R. Lutz, S. Nanda, S. Niemejer, A. Pazmiño, G. Pinardi, J.-P. Pommereau, A. Richter, N. Rozemeijer, M.K. Sha, D. Stein Zweers, N. Theys, G. Tilstra, O. Torres, P. Valks, C. Vigouroux, and P. Wang: S5P MPC Routine Operations Consolidated Validation Report series, Issue #05, Version 05.0.1, 151 pp., December 2019.

Lelieveld, J., Gromov, S., Pozzer, A., and Taraborrelli, D.: Global tropospheric hydroxyl distribution, budget and reactivity, Atmos. Chem. Phys., 16, 12477–12493, https://doi.org/10.5194/acp-16-12477-2016, 2016.

Myhre, G., Shindell, D., Bréon, F.-M., Collins, W., Fuglestvedt, J., Huang, J., Koch, D., Lamarque, J.-F., Lee, D., Mendoza, B., and Nakajima, T.: Anthropogenic and natural radiative forcing, Climate Change, 423, 658–640, 2013.

Ostler, A., Sussmann, R., Rettinger, M., Deutscher, N. M., Dohe, S., Hase, F., Jones, N., Palm, M., and Sinnhuber, B.-M.: Multistation intercomparison of column-averaged methane from NDACC and TCCON: impact of dynamical variability, Atmos. Meas. Tech., 7, 4081–4101, https://doi.org/10.5194/amt-7-4081-2014, 2014.

Rigby, M., Montzka S.A, Prinn, R.G., White, J.W.C., Young, D., O'Doherty. S., Lunt, M.F., Ganesan, A.L., Manning, A.J., Simmonds, P.G., Salameh, P.K., Harth, C.M., Mühle, J., Weiss, R.F., Fraser, P.J., Steele, L.P., Krummel, P.B., McCulloch A., Park., S.: Role of OH in recent methane growth. Proceedings of the National Academy of Sciences, 114 (21) 5373-5377; DOI: 10.1073/pnas.1616426114, 2017.

Rodgers, C. D.: Inverse methods for atmospheric sounding: theory and practice, vol. 2 of Series on atmospheric, oceanic and planetary 335 physics, World Scientific, Singapore, 2000.

Rodgers, C. D. and Connor, B. J.: Intercomparison of remote sounding instruments, J. Geophys. Res.-Atmos., 108, 4116–4229, doi:10.1029/2002JD002299, 2003.

Sha, M. K. and Langerock, B.: S5P MPC VDAF and TCCON4S5P CH4 validation results, presentation at the Sentinel-5P Third products Release Workshop, https://sentinel.esa.int/documents/247904/3753563/S5PCH4-VAL-MPC-TCCON4S5P, 2019a.

Sha, M. K., De Mazière, M., Notholt, J., Blumenstock, T., Chen, H., Dehn, A., Griffith, D. W. T., Hase, F., Heikkinen, P., Hermans, C., Hoffmann, A., Huebner, M., Jones, N., Kivi, R., Langerock, B., Petri, C., Scolas, F., Tu, Q., and Weidmann, D.: Intercomparison of low and high resolution infrared spectrometers for ground-based solar remote sensing measurements of total column concentrations of CO2, CH4 and CO, Atmos. Meas. Tech. Discuss., https://doi.org/10.5194/amt-2019-371, in review, 2019b.

Toon, G. C.: The JPL MkIV interferometer, Opt. Photon. News, 2, 19–21, doi:10.1364/OPN.2.10.000019, 1991.

Toon, G. C. and Wunch, D.: A stand-alone a priori profile generation tool for GGG2014 release (Version GGG2014.R0). CaltechDATA. https://doi.org/10.14291/tccon.ggg2014.priors.r0/1221661, 2017

Veefkind, J., Aben, I., McMullan, K., örster, H., de Vries, J., Otter, G., Claas, J., Eskes, H., de Haan, J., Kleipool, Q., vanWeele, M., Hasekamp, O., Hoogeveen, R., Landgraf, J., Snel, R., Tol, P., Ingmann, P., P., V., Kruizinga, P., Vink, R., Visser, H., and Levelt, P.: TROPOMI on the ESA Sentinel-5 Precursor: A GMES mission for global observations of the atmospheric composition for climate, air quality and ozone layer applications, Remote Sens. Environ., 120, 70–83, doi:10.1016/j.rse.2011.09.027, 2012.

Vogel, F., Frey, M., Staufer, J., Hase, F., Broquet, G., Xueref-Remy, I., Chevallier, F., Ciais, P., Sha, M.K., Chelin, P., Jeseck, P., Janssen, C., Te, Y., Groß, J., Blumenstock, T., Tu, Q., Orphal, J.: XCO2 in an emission hot- spot region: the COCCON Paris campaign 2015, Atmospheric Chemistry and Physics, doi: 10.5194/acp-19-3271-2019, 2019

Wang, Y., Ma, Y.-F., Eskes, H., Inness, A., Flemming, J., and Brasseur, G. P.: Evaluation of the CAMS global atmospheric trace gas reanalysis 2003–2016 using aircraft campaign observations, Atmos. Chem. Phys. Discuss., https://doi.org/10.5194/acp-2019-821, in review, 2019.

World Meteorological Organization, 2019: WMO Greenhouse Gases Bulletin: The State of Greenhouse Gases in the Atmosphere Based on Global Observations through 2018. No. 15, https://library.wmo.int/doc_num.php?explnum_id=10100

Wunch, D., Toon, G. C., Blavier, J.-F. L., Washenfelder, R. A., Notholt, J., Connor, B. J., Griffith, D. W. T., Sherlock, V., and Wennberg, P. O.: The total carbon column observing network, Philos. T. R. Soc. A, 369, 2087–2112, doi:10.1098/rsta.2010.0240, 2011.

Wunch, D., Toon, G. C., Sherlock, V., Deutscher, N. M., Liu,C., Feist, D. G., and Wennberg, P. O.: The Total CarbonColumn Observing Network's GGG2014 Data Version, Tech.rep., California Institute of Technology, Carbon Dioxide In-formation Analysis Center, Oak Ridge National Laboratory,Oak Ridge, Tennessee, USA, https://doi.org/10.14291/tccon.ggg2014.documentation.R0/1221662, 2015.

Wunch, D., Wennberg, P. O., Osterman, G., Fisher, B., Naylor, B., Roehl, C. M., O'Dell, C., Mandrake, L., Viatte, C., Kiel, M., Griffith, D. W. T., Deutscher, N. M., Velazco, V. A., Notholt, J., Warneke, T., Petri, C., De Maziere, M., Sha, M. K., Sussmann, R., Rettinger, M., Pollard, D., Robinson, J., Morino, I., Uchino, O., Hase, F., Blumenstock, T., Feist, D. G., Arnold, S. G., Strong, K., Mendonca, J., Kivi, R., Heikkinen, P., Iraci, L., Podolske, J., Hillyard, P. W., Kawakami, S., Dubey, M. K., Parker, H. A., Sepulveda, E., García, O. E., Te, Y., Jeseck, P., Gunson, M. R., Crisp, D., and Eldering, A.: Comparisons of the Orbiting Carbon Observatory-2 (OCO-2) XCO2 measurements with TCCON, Atmos. Meas. Tech., 10, 2209–2238, https://doi.org/10.5194/amt-10-2209-2017, 2017.